Liposomal Fe(III) Macrocyclic Complexes with Hydroxypropyl Pendants as MRI probes

*Samira M. Abozeid,[a, b] Md Saiful I. Chowdhury,[a] Didar Asik,[a] Joseph A. Spernyak,[c] and Janet R. Morrow[a]**

[a] Department of Chemistry, University at Buffalo, The State University of New York Amherst, NY 14260, United States

[b] Department of Chemistry, Faculty of Science, Mansoura University, El-Gomhoria Street, 35516 Mansoura, Egypt

[c] Department of Cell Stress Biology, Roswell Park Comprehensive Cancer Center, New York 14263 United States

*E-mail: jmorrow@buffalo.edu

ABSTRACT: Paramagnetic liposomes containing Fe(III) complexes were prepared by incorporation of mononuclear (Fe(L1) or Fe(L3)) or dinuclear (Fe_2(L2)) coordination complexes of 1,4,7-triazacyclononane macrocycles containing 2-hydroxypropyl pendant groups. Two different types of paramagnetic liposomes were prepared. The first type, LipoA, has the mononuclear Fe(L1) complex loaded into the internal aqueous core. The second type, LipoB, has the amphiphilic Fe(L3) complex inserted into the liposomal bilayer and the internal aqueous core loaded with either Fe(L1) (LipoB1), or Fe_2(L2) (LipoB2). LipoA enhances both T_1 and T_2 water proton relaxation rates. Treatment of LipoA with osmotic gradients to produce a non-spherical liposome produces a liposome with a chemical exchange saturation transfer (CEST) effect as shown by an asymmetry analysis, but only at high osmolarity. LipoB1, which contains an amphiphilic complex in the liposomal bilayer produced a broadened Z-spectrum upon treatment

of the liposome with osmotic gradients. The r_1 relaxivity of LipoB1 and LipoB2 were higher than the r_1 relaxivity of LipoA on a per Fe basis, suggesting an important contribution from the amphiphilic Fe(III) center. The r_1 relaxivities of paramagnetic liposomes are relatively constant over a range of magnetic field strengths (1.4 T to 9.4 T), with the ratio of r_2/r_1 substantially increasing at high field strength. MRI studies of LipoB1 in mice showed prolonged contrast enhancement in blood compared to the clinically employed Gd(DOTA), which was injected at 2-fold higher dose per metal than the Fe(III) loaded liposomes.

Keywords: liposome, iron coordination complexes, magnetic resonance imaging contrast agent

INTRODUCTION

Liposomes are small bilayer vesicles of typically 100 to 400 nm in size that are formed from phospholipids.[1-3] Liposomes are commonly used to encapsulate small molecules within their hydrophilic interior core for biomedical applications such as the transport of small molecule drugs in vivo.[4, 5] Liposomes have biodistribution profiles that are distinct from those of small molecules and thus may improve the pharmacokinetic profile of the drug.[6] For example liposomes, as examples of nanoparticles, accumulate in tumors by the enhanced permeability retention effect.[3] Moreover, targeting of liposomes to specific tissues may be enhanced by the attachment of peptides or antibodies to the lipid polar head groups.[5, 7] In these studies, it is useful to track the biodistribution of the liposome and the corresponding delivery of the drug cargo by adding imaging probes to the liposome.[6, 8-11] Such a theranostic approach is desirable to combine drug treatments with a diagnostic procedure.[6, 12, 13] As for choices of diagnostic options, Magnetic Resonance Imaging (MRI) is one of the most powerful procedures used clinically, due to its

unlimited depth penetration and high resolution.[14, 15] A paramagnetic metal complex is added to the liposome to facilitate its tracking through MRI. Paramagnetic liposomes enhance the MR image through enhanced T_1 or T_2 water proton relaxation rates[5, 9, 13, 16] or alternatively, by production of a chemical exchange saturation transfer (CEST) effect.[17]

Gd(III) complexes are the most frequently used for production of paramagnetic liposomes. Typically, an alkyl chain is added to the Gd(III) complex to incorporate it into the lipid bilayer.[3, 8, 11, 17] This places Gd(III) complexes at the bulk water interface for more effective water proton relaxation. If the Gd(III) complex is anchored rigidly to the liposome through careful placement of more than one alkyl chain, enhanced T_1 proton relaxation may result from a longer rotational correlation time of the Gd(III) center in the liposomal nanoparticle.[18] Alternatively, the free Gd(III) complex may be encapsulated in the liposomal interior or core. In this case, the proton relaxation per Gd(III) may be quenched due to slow exchange of the water molecules through the lipid bilayer relative to the rate of proton relaxation of the water molecules surrounding the Gd(III) complex.[18-20]

Alternatively, liposomes containing other lanthanides including Tm(III), Dy(III), Eu(III) or Yb(III) may produce a shift of the intraliposomal water proton resonances to produce a CEST effect in a process that involves exchange of the interior water molecules with the bulk water.[17, 21, 22] The paramagnetic complexes in such lipoCEST agents shift the water proton resonances in the interior of the liposome away from that of the bulk water. Irradiation of the interior water protons with a presaturation radiofrequency pulse followed by exchange through the liposomal membrane leads to a CEST effect that can be used for imaging.[17] LipoCEST agents have the advantage of much higher sensitivity due to the large number of intraliposomal water molecules compared to simple paraCEST agents and have been shown to produce detectable signal at nanomolar

concentrations.[17] While the most common choice of paramagnetic metal center for lipoCEST agents features Ln(III) with large magnetic anisotropies such as Dy(III), Yb(III) and Tm(III),[8, 11, 21, 22] a transition metal lipoCEST agent has been recently reported.[23] This agent contains two different high spin Co(II) complexes which produce some of the largest water proton shifts reported to date for transition metal complexes.[23-25] When loaded into liposomes, Co(II) complexes produce lipoCEST agents. However, even metal ions with isotropic distribution of unpaired f-electrons such as Gd(III) may produce lipoCEST agents if liposomes of oblong shapes are used.[26] In this case, there is a bulk magnetic susceptibility contribution that gives rise to an additional shift of the proton resonance of the intraliposomal water. Such non-spherical liposomes are produced by treating the liposomes with an osmotic gradient. Incubation of the liposome in a solution of greater osmolarity than that on the inside results in a leakage of the water molecules from the liposome and a corresponding change in shape.[22] Thus, liposomes that are core-loaded with Gd(III) complexes may behave as T_1, T_2 or CEST agents, a three in one probe.[26]

High-spin Fe(III) complexes enhance proton relaxation rates and are of interest as alternatives to Gd(III) contrast agents.[27-33] A potential advantage in the development of iron-based coordination complexes arises from iron's status as the most abundant transition metal in the human body and the availability of biological pathways in humans for recycling and storage of iron.[34, 35] Here we introduce some of the first examples of liposomes loaded with high spin Fe(III) macrocyclic complexes. Most other examples of iron-loaded liposomes contain superparamagnetic iron oxide nanoparticles (SPIONs).[36-38] An earlier example of iron coordination complexes featured deferoxamine Fe(III) derivatives loaded inside of a liposome.[6] An additional early report that used a long chain derivative of DTPA (diethylenetriamine pentaacetate) to coordinate Fe(III) failed to produce stable liposomes whereas Mn(II) or Gd(III) analogs were stable.[39] Our goal here

was to prepare some of the first stable iron complex-based liposomes and to study both encapsulated complexes and complexes incorporated into the bilayer. Liposomes with encapsulated complex are of interest as MRI probes that respond to temperature or pH changes to release the encapsulated complex.[5, 11, 40] Liposomes with paramagnetic complex incorporated into the bilayer are of interest as enhanced T_1 , T_2 or lipoCEST MRI probes.[5, 7-10, 18, 39]

The coordination complexes studied here are members of a new class of high spin Fe(III) complexes with macrocyclic ligands that are effective T_1 MRI probes.[28, 41, 42] Members of this class of compounds produce r_1 relaxivity values that are comparable to Gd(III) agents in serum and show enhanced contrast in mice at 4.7 T.[28] These macrocyclic complexes are part of a larger recent effort to develop Fe(III) coordination complexes as alternatives to the current clinically used Gd(III) contrast agents.[27, 30] Some of the new Fe(III) contrast agents lack an exchangeable water ligand, yet still show pronounced r_1 proton relaxivity through second-sphere interactions.[28, 43] The better-known Fe(III) coordination complexes that are seven-coordinate and contain linear polyaminocarboxylate ligands and an exchangeable inner-sphere water ligand have been studied for many years,[30, 33] however, improved derivatives have been recently reported.[29, 44] Such classical Fe(III) complexes have been recently analyzed in detail through nuclear magnetic dispersion studies and theoretical calculations to elucidate contributions to proton relaxivity.[45]

Two different types of liposomes are studied here including LipoA with internally loaded Fe(III) coordination complex, and LipoB with internally loaded Fe(III) complex and an amphiphilic Fe(III) complex that incorporates into the bilayer.[17] Two of the Fe(III) complexes lack an inner-sphere water,[42] but have protons on the hydroxypropyl groups to facilitate second sphere water interactions or proton-exchange based T_1 relaxation.[46] The dinuclear Fe(III) complex has one bound water per iron center.[41] LipoA and LipoB are studied as T_1 and T_2 MRI probes. The

potential of these paramagnetic liposomes to produce LipoCEST agents is studied as a third contrast mechanism. The liposome with the highest r_1 relaxivity per particle was chosen to study as an MRI contrast agent in mice.

Scheme 1. Schematic of LipoA and LipoB. The predominant Fe(III) complex species in this study are shown in their protonation state at neutral pH.

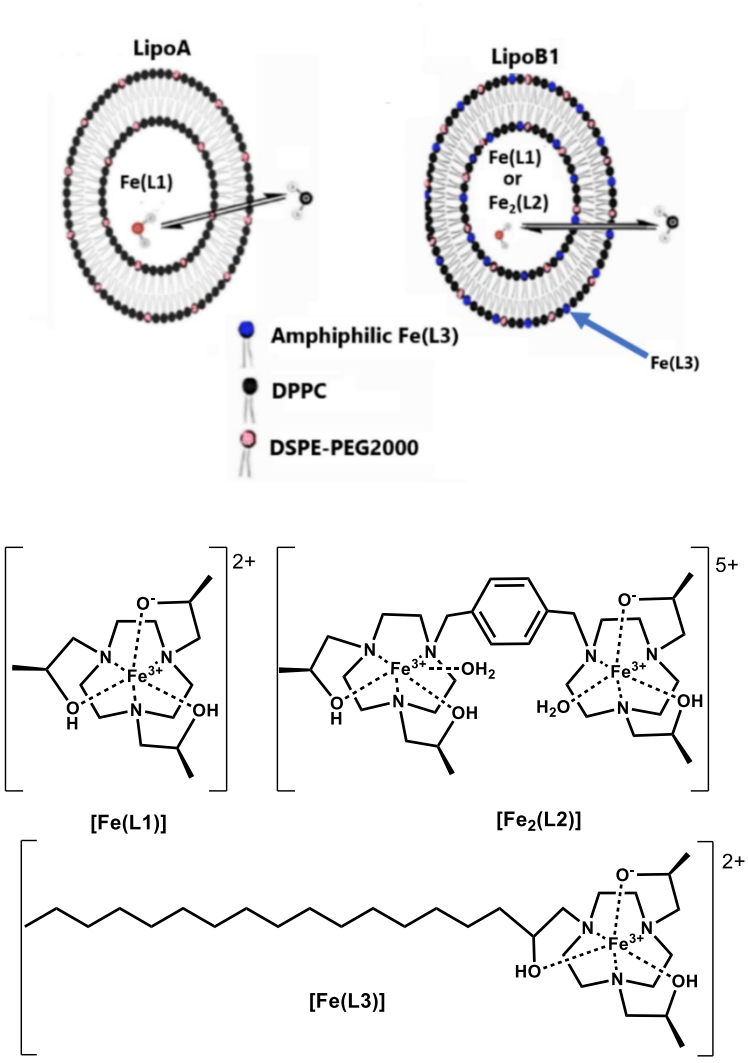

EXPERIMENTAL SECTION

Instrumentation. A Varian Inova 500 MHz NMR spectrometer (11.7 T) equipped with FTS Systems TC-84 Kinetics Air Jet Temperature Controller was used to collect ^{1}H NMR spectra. ^{13}C NMR spectra were acquired using a Varian Mercury 300 MHz or 400 MHz NMR spectrometer. Proton relaxivity experiments were performed at 1.4 T (34 ºC) on a Nananalysis NMR spectrometer, at 4.7 T (37 ºC) on a Bruker preclinical MRI scanner or at 9.4 T, (37 ºC) on a Varian Inova 400 MHz NMR spectrometer. Z-spectra were collected on a Varian Inova 500 MHz NMR spectrometer (11.7 T). All pH measurements were made by utilizing an Orion 8115BNUWP Ross Ultra Semi Micro pH electrode connected to a 702 SM Titrino pH. ThermoFinnigan LCQ Advantage IonTrap LC/MS equipped with a Surveyor HPLC system was used to for mass spectrometry data of the complexes. Iron concentration was determined by using a Thermo X-Series 2 ICP-MS as reported.[42, 47]

Chemicals. DPPC, DSPE-PEG2000, and cholesterol were purchased from Avanti Polar Inc. (Alabaster, Al, USA). The L1 and L2 ligands, and their iron complexes, $[Fe_2(L2)Cl_2]Cl_2$ and $Fe(L1)Cl_2$, and were prepared as reported.[41, 42]

Synthesis of L3. In a 10 mL round-bottom flask, (2S,2'S)-1,1'-(1,4,7-triazonane-1,4-diyl)bis(propan-2-ol) (0.2 g, 0.82 mmol)[28] was dissolved in 5.0 mL of absolute ethanol. To this solution was added racemic 2-hexadecyloxirane (1.22 mmol, 1.5 equiv). After the solution was stirred at 60 ºC for 3 days, the solvent was removed under pressure to yield a pale-yellow powder. The crude product was then dissolved in methanol or ethanol, and any precipitate was removed by filtration. The filtrate was dried under reduced pressure to yield (2S,2'S)-1,1'-(7-(2-hydroxyoctadecyl)-1,4,7-triazonane-1,4-diyl)bis(propan-2-ol) with 80% yield. **ESI-MS:** *m/z* 514.50 ($M+H^+$, 100%) where M = L3. **^{1}H NMR:** (400 MHz, $CDCl_3$): δ 4.40 (3H, -O**H**), δ 2.61,

2.58 (6H, -C**H**$_2$-NH- hydroxylpropyl pendants), δ 3.76,3.52 (3H, -**C**H alcohol pendent), δ 2.79, 2.65 (12H, -C**H**$_2$ macrocycle), δ 1.08 (6H, -C**H**$_3$) and δ 0.87, 1.25, 1.24 (protons of two long chain carbon). **^{13}C NMR** (300 MHz, $CDCl_3$): δ 14.08, 22.68 (3C, -**C**H_3), δ 51.01 (6C, macrocycle ring), δ 74.92, 70.34 (3C, -**C**H alcohol pendent), δ 67.34, 64.61 (3C, -**C**H_2-NH- alcohol pendents), and δ 37.81, 33.14, 31.91, 29.67, 29.35, 25.53 (15C, -**C**H_2 long chain carbon).

The **Fe(L3)** complex was synthesized by dissolving L3 (0.15 mmol) in ethanol and heating the solution to 60°C. Iron(II) chloride (1-2 equivalents) was dissolved in ethanol (2.0 mL) and was added dropwise to the ethanolic ligand solution in which the product precipitated as a yellow solid. The solution was allowed to stir overnight, then filtered and the product was washed with ethanol. The **[Fe(L3-H+)]Cl** complex was isolated as a brownish-orange solid in 55% yield. ESI-MS of [Fe(L3-H+)]Cl: m/z = 567.4 [M^+] 589.5 [$M+Na^+$] and 1155 [$2M+Na^+$]. Percent iron through ICP-MS analysis: 94%. Here M^+ is [Fe(L3-2H^+)].

Magnetic susceptibility. The effective magnetic moments (μ_{eff},) of the complexes or paramagnetic liposomes were determined by ^{1}H NMR by using the Evans method.[48, 49] Samples were prepared using a coaxial NMR insert which contained the diamagnetic standard of 5 % t-butanol in D_2O. Evans method was used to determine the effective magnetic moment of Fe(III) complexes and as a way to determine the concentration of Fe(III) complexes in the liposomes as reported previously for Co(II) loaded liposomes.[23]

Liposomes preparation and characterization. Liposome Type A (LipoA) was prepared using the previously reported ethanol injection method with some modifications.[23] The hydration solution was 40-50 mM of Fe(III) complex, pH 6.8-7.2, adjusted using meglumine solution and total lipid content was 20 mg/mL. The bilayer was composed of DPPC/Cholesterol/DSPE-PEG2000 with a molar ratio of 55:40:5. To reduce the size, the liposome suspension was passed

12 times at 60 °C through sequentially stacked polycarbonate membranes of 100 nm and 6 times through 80 nm pore size using an Avanti mini-extruder with heating block. Non-encapsulated complex was eliminated by exhaustive dialysis at 4 ºC. Shrunken liposomes were prepared by dialysis against different concentrations of HEPES/NaCl buffer pH 7-7.2. The Fe concentration was determined by using ICP-MS and/or NMR spectroscopy by measuring bulk magnetic susceptibility (Evans Method).[48]

Liposome type B (LipoB) was prepared using the liposomal formulation of DPPC/DSPE-PEG2000/Cholesterol/Amphiphilic Fe(L3) (molar ratio of 54:6:30:10). LipoB was made by dissolving the lipid mixture in chloroform/methanol, then evaporating the solution to dryness under vacuum to produce thin lipid film formation. The thin film was hydrated with an aqueous solution (1 mL) containing 50 mM of the hydrophilic complex; Fe(L1) or Fe_2(L2) at 50 ºC. The pH of the iron complex containing solution was raised to the desired pH by adding meglumine. The solution was stirred for 90 minutes at 50 °C followed by stirring at 25 ºC for 90 minutes. The liposome suspension was then extruded to reduce the size by passing 20 times through polycarbonate membranes of 200 nm using the Avanti mini extruder with the heating block. To remove any free complex, the liposome suspension was dialyzed against 300 mOsm/L of NaCl aqueous solution and HEPES buffer pH 6.8-7.2 at 4º C. Alternatively, the liposomes were isolated and washed by using ultrafiltration. The liposomal suspension was washed with 300 mOsm/L of NaCl aqueous solution using Amicon 100 KDa ultra-filtration kit. The first filtrate was saved to calculate the entrapped iron complex inside liposomal core using UV-vis spectroscopy. In these studies, the electronic absorbance of Fe(L1) filtrate at 330 nm was compared to that of aqueous Fe(L1) solution[42] for thin film hydration during liposome formulation. The liposomal solution was then sequentially washed five more times using the same ultra-centrifugal filtration kit to remove

free Fe(L1) complex. The mean hydrodynamic liposome diameter was determined by dynamic light scattering. The iron content was determined by ICP-MS. All liposomes were stored at 4 ^{o}C.

Water proton relaxation time measurements. Experiments were performed at several magnetic field strengths including 1.4 T (34 ^{o}C), 4.7 T (37 ^{o}C) or at 9.4 T, (37 ^{o}C). Several different concentrations were prepared by diluting either iron complexes (non-liposomal system) or liposomes, then the sample was placed into a coaxial tube insert and placed in an NMR tube filled with DMSO-d_6. The T_1 proton relaxation measurement was run on liposomes in the absence of the paramagnetic complexes as well. The T_1 proton relaxation times of solutions containing complex or liposomes were measured on a 9.7 T NMR spectrometer at 37 °C using the inversion recovery method with the following parameters: relaxation delay = 15-20 s, echo time array starting from 0.2–5 s, and a receiver bandwidth = 28 ms. T_2 relaxation times were measured using the Carr–Purcell–Meiboom–Gill (CPMG) spin echo method. The CPMG sequence was used with a fixed TR of 10 s and TE times ranging from 0.02–4 ms in 0.1 s increments.

Z-spectra. In general, the Z-spectra of shrunken liposomes were acquired at 37 ^{o}C at 11.7 T with varied pre-saturation pulse power (B_1) applied for 2 seconds, and the frequency offset was varied in either 500 or 250 Hz increments. The Z-spectrum was obtained by plotting normalized water intensity against offset frequency. The aqueous liposome sample was placed into a coaxial tube insert, within an NMR tube filled with DMSO-d_6.

Mice imaging studies. MR imaging studies with the Fe(III)-based liposomes and complexes were studied on at 4.7 T Bruker preclinical MRI in healthy mice (BALB/cJ, Jackson Laboratory). Solutions were formulated with Fe(III) complex loaded liposomes at 20 mg lipids/mL. To study enhancement kinetics, serial T_1-weighted, 3D, spoiled-gradient echo scans (TE/TR = 3/15ms, flip angle = 40°) covering the mouse from thorax to tail were acquired prior to

and after administration of compounds. NMR tubes loaded with 1% agarose doped with $CuSO_4$ were used for MRI signal normalization. Animals were dosed with 25 μmol [Fe]/ kg intravenously via tail vein and MR data were recorded continuously for up to 1 hour, and additionally at 4 hours post-administration. For comparison, FDA-approved MRI contrast agent gadoterate meglumine (Gd-DOTA, Dotarem®) was injected at 50 μmol [Gd]/kg into a separate group of mice. Signal intensities were normalized to the phantoms, and signal increase in each organ was measured. Studies were carried out in triplicate (n=3) for each compound tested.

RESULTS AND DISCUSSION

The development of Fe(III) complexes that are of sufficient solubility for liposome encapsulation, typically 40-100 mM, in aqueous solution is a challenge. Moreover, the slow kinetics of ligand exchange involved in the formation of Fe(III) complexes makes it difficult to obtain complexes by adding Fe(III) salts to already prepared liposomes. For example, previous research that failed to form stable liposomes containing an amphiphilic Fe(III) DTPA derivative in water added Fe(III) salts in the last step.[39] In studies here, the Fe(III) complexes are formed first and then incorporated into the liposomes. The complex aqueous solution chemistry of Fe(III) may also be problematic as complexes with a bound water may undergo dimerization to produce a u-oxo bridged dimers.[44] For this reason, we chose to use Fe(III) complexes of the 1,4,7-triazacyclononane (TACN) macrocycle. The complexes contain hydroxypropyl pendants to stabilize the iron center as high spin Fe(III). In complexes with open coordination sites, the hydroxypropyl pendants inhibit dimerization and produce complexes of moderately high solubility in water.[28] This class of complexes is inert towards dissociation in the presence of physiologically

relevant concentrations of phosphate and carbonate or in solutions containing 100 mM HCl, at 37 °C over a period of several hours to days.[41, 42]

The Fe(L1) and Fe(L3) complexes are six-coordinate and lack an inner-sphere water ligand, whereas the dinuclear complex (Fe_2(L2)) has a coordination site for bound water on each Fe(III) center.[41, 42] The proton r_1 relaxivity of Fe(L1) is attributed predominately to second-sphere and outer-sphere water interactions (Table 1, Figure S1).[42, 46] Notably, the dinuclear Fe(III) complex has a 2.6-fold greater relaxivity per molecule compared to Fe(L1) at 4.7 T. The greater relaxivity of the Fe(III) centers of the dinuclear complex is attributed to the open coordination sites that allow for an inner-sphere water molecule. Notably, the exchange of the inner-sphere water on Fe_2(L2) is slow on the NMR time scale, yet the complex still produces higher relaxivity than complexes that lack the bound water.[41] The r_1 relaxivity of the dinuclear complex is also expected to be larger than the mononuclear complex due slower tumbling times and by the presence of two Fe(III) centers. Fe(L3) contains a long alkyl chain to give an amphiphilic complex for incorporation into the liposomal bilayer. Notably, all complexes are cationic at neutral pH (Scheme 1) as determined by studies using pH-potentiometric titrations.[28, 41, 42]

LipoA studies. The first type of liposome studied, LipoA, was prepared by encapsulating Fe(L1) into the liposomal interior. The hydration solution contained 40-50 mM of Fe(III) complex, pH 6.8-7.2 and total lipid content was 20 mg/mL. The bilayer was composed of DPPC/Cholesterol/DSPE-PEG2000 with a molar ratio of 55:40:5. PEGylated liposomes were used to prevent vesicle aggregation[50] and to increase the blood circulation time by decreasing the extent elimination through the hepatobiliary system in mice.[2, 5, 51] The relatively high percentage of cholesterol was used to reduce PEG chain interactions[52] and to modulate the water exchange rate constants.[53] The total Fe(III) content was determined by ICP-MS of liposomes and filtrate

and by measurement of magnetic susceptibility by using the Evans method.[21, 48] Despite the high concentration of complex used to make the liposomes, the concentration of the complex inside the liposomes ranged from 8-10 mM Fe(L1).

The T_1 proton relaxation times of the LipoA liposomes were measured as a function of liposomal size for three different sizes. The r_1 relaxivity decreased as the liposome size increased ranging from 0.50 $mM^{-1}s^{-1}$ to 1.0 $mM^{-1}s^{-1}$ (Table S2, Figure S2), consistent with the expected decrease in surface/volume ratio for larger liposomes. Larger surface to volume ratios of small liposomes favor higher rates of water exchange between the intraliposomal and extraliposomal water molecules.[54] Thus, the quenching of r_1 relaxivity observed for larger-sized LipoA (208 and 380 nm), is attributed to slowed water exchange through the lipid bilayer compared to the proton water relaxation rate of free complex.[55] By comparison, the r_1 relaxivity of the free Fe(L1) complex at 1.5 $mM^{-1}s^{-1}$ at 1.4 T, 34 °C was higher than that for any of the LipoA formulations on a per iron basis.

The magnetic field strength dependence of the r_1 relaxivity of LipoA shows a 20 % increase on going from 1.4 T to 4.7 T, but little change at higher field strengths. This trend is similar to that observed for simple coordination complexes of Fe(III). Unlike Gd(III) complexes, Fe(III) macrocyclic complexes do not show the trend of decreasing relaxivity at high field strengths.[41] Full field strength dependence in the form of nuclear magnetic dispersion (NMRD) studies on iron coordination complexes are scarce, but increasing interest in Fe(III) contrast agents has brought renewed effort in this endeavor.[45, 56, 57] An explanation for the trend for Fe(III) complexes is that the relatively fast electronic relaxation times of the Fe(III) centers are better suited for the higher field strengths that are studied here.[58] On the other hand, the r_2 relaxivity of LipoA increases substantially at 9.4 T. The increase of r_2 relaxivity with field strength is predicated on the large

field strength dependence of the magnetic susceptibility contribution to r_2.[9] Thus the r_2/r_1 ratio increases from 2.3 at 1.4 T to 7.3 at 9.4 T for LipoA.

Table 1. The r_1 and r_2 relaxivity values for liposomes and complexes at 4.7, 9.4 T (37 ºC) and 1.4 T (34 °C) and pH 6.8-7.2.

AGENT	r_1($mM^{-1}s^{-1}$) 1.4 T	r_1($mM^{-1}s^{-1}$) 4.7 T	r_1($mM^{-1}s^{-1}$) 9.4 T	r_2($mM^{-1}s^{-1}$) 1.4 T	r_2($mM^{-1}s^{-1}$) 4.7 T	r_2($mM^{-1}s^{-1}$) 9.4 T
Fe(L1)[a]	1.5 ± 0.2	0.97± 0.12	1.4± 0.1	-	1.8± 0.5	-
Fe_2(L2)[b]	3.5± 0.3	5.3± 0.1	4.0 ± 0.3	-	13.0± 0.2	-
LipoA[c]	0.84± 0.15	0.92± 0.20	1.2± 0.1	2.0± 0.2	1.6± 0.3	8.7± 1.0
LipoB1	1.7 ± 0.3	1.7± 0.4	2.1± 0.2	2.8± 0.3	9.4± 0.9	20 ± 3

a. Data at 1.4 and 4.7 T from references.[42, 46] b. from reference.[41] c. for liposomes of 126 nm size.

LipoA was also studied as a lipoCEST agent by recording the Z-spectra as shown in Figure 1. LipoCEST agents have intraliposomal water proton resonances that are shifted from that of bulk water by the paramagnetic complexes trapped in the interior of the liposome.[17] For metal ions with magnetic anisotropy arising from the asymmetrical distribution of electrons in the d or f orbitals, such as Co(II) or Tm(III), respectively, the intraliposomal water proton shift is

a result of the hyperfine contribution which arises from to the interaction between the intraliposomal water protons and the paramagnetic center.[21] In contrast, metal ions with an isotropic distribution of electrons including high spin Fe(III) complexes or Gd(III) complexes are not expected to produce a hyperfine shift of the water protons in spherical liposomes. However, a liposome loaded with a paramagnetic complex which is not spherical, but is oblong in shape, is expected to have a bulk magnetic susceptibility contribution (**Eq. 1**). Here $\Delta_{intraliposomal}$ is the chemical shift difference between intraliposomal and bulk water protons, Δ_{Hyp} is the contribution from the hyperfine shift of the paramagnetic complex and Δ_{BMS} is the bulk magnetic susceptibility shift. Thus, Gd(III) complexes in non-spherical liposomes have been shown to shift the water proton resonances away from that of bulk water and to exhibit a lipoCEST effect.[26] Similarly, high spin Fe(III) as an isotropic metal ion would be expected to show a negligible CEST effect when loaded in a symmetrical liposome, but potentially exhibit a CEST effect in an oblong shaped liposome.[22]

$$\Delta_{Intralipo} = \Delta_{HYP} + \Delta_{BMS} \qquad \boldsymbol{Eq.1}$$

Shrinkage of the Fe(III)-based LipoA produced a Z-spectrum with a shoulder at about 5ppm as presented in Figure 1 and Figures S3-S5. Shrunken liposomes were prepared by applying osmotic stress through dialysing the liposome suspension against different concentrations of NaCl and HEPES buffer to change the shape of the liposome from spherical to oblong.[21, 59] The shoulder on the Z-spectrum was pronounced only at high osmotic stress (600-1200 mOsm/L), which is larger than that found under physiological conditions (300 mOsm/L). Given the small difference between the bulk water proton resonance and the intraliposomal water proton resonance $\Delta\omega$, the magnetization transfer asymmetry (MTR_{asym}) profile was plotted in

Figure S5 to better analyze the effect.[60] The small frequency offset centered at 4 ppm associated with the MTR_{asym} plot is attributed to the low concentration of Fe(III) complex and to the isotropic state of the Fe(III) ion. Gd(III) loaded liposomes similarly showed small intraliposomal water proton shifts (7 ppm at 300 mOsm/L) that were not as large as that of other lanthanide shift agents.[26] The frequency offset for the CEST shoulder that we observe here for Fe(III) loaded liposomes is also less than that observed with Co(II) loaded liposomes, as an additional example of a transition metal probe. Co(II) macrocyclic complexes are effective water proton shift agents and produce a LipoCEST peak at about 10 ppm with complexes loaded into the liposome interior.[23]

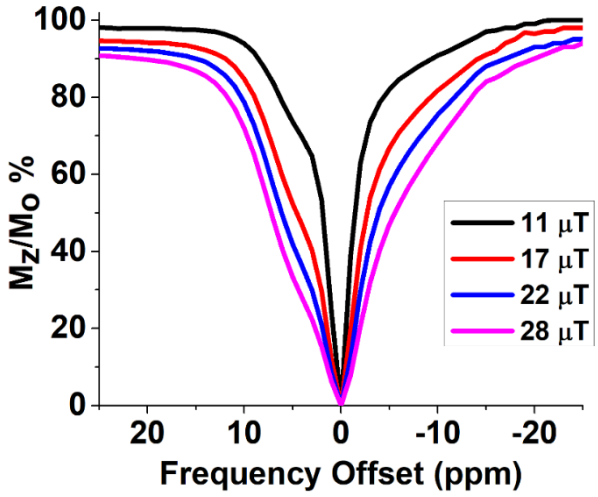

Figure 1: Z-spectrum of LipoA, which is core loaded with Fe(L1), at 1200 mOsm/L, at 37 °C, pH 6.8, 11.7 T.

LipoB studies. To enhance the relaxivity of the iron liposomes, an amphiphilic iron complex was added to the bilayer while keeping the liposomal interior filled with complex. We anticipated that LipoB agents would have a large per particle relaxivity with the two different types of Fe(III) complexes. LipoB was prepared with Fe(L3) as an amphiphilic agent inserted in the liposomal bilayer and with the aqueous cavity (lumen) loaded with either Fe(L1) complex (LipoB1) or with Fe_2(L2) (LipoB2). A liposomal formulation comprised of 40 mM total lipid - DPPC/DSPE-PEG2000/Cholesterol/Amphiphilic Fe(L3) (molar ratio of 54:6:30:10) was used, which is similar to that of LipoA, but with the addition of the amphiphilic complex. LipoB was made by dissolving the lipid mixture in chloroform/methanol, then evaporating the solution to dryness under vacuum to produce thin lipid film formation. The thin film was hydrated with an aqueous solution (1 mL) containing 50 mM of the hydrophilic complex; Fe(L1) or Fe_2(L2) at 50 °C. The sizes of LipoB1 and LipoB2 were 190 nm and 180 nm, respectively as measured by

dynamic light scattering. The overall iron content was determined by ICP-MS and showed that there was almost three-fold more iron per liposome in LipoB2 than in LipoB1. Calculations of iron per liposome particle give the equivalent of 12 mM iron for LipoB1 and 30 mM iron for LipoB2, which includes both the internal and the liposomal surface Fe(III) content. Assuming that the lipid bilayer in both LipoB1 and LipoB2 contains the 10% of amphiphilic Fe(III) complex, the higher concentration of iron in LipoB2 suggests that a higher loading efficiency is obtained with the dinuclear complex. A higher loading efficiency was observed previously for liposome containing multinuclear lanthanide complexes[17, 61, 62] and suggests that this method will be successful for Fe(III) complexes as well.

The proton relaxivity of the paramagnetic liposomes (LipoB) has three contributions including from iron centers in the external liposomal layer (C_{out}), and C_{in} which corresponds to the concentration of iron centers embedded in the internal layer that directly interact with the intraliposomal water protons. In addition, there is the internal component which is related to the amount of hydrophilic agent in the liposomal internal aqueous cavity. If the water exchange rate through the liposomal membrane is sufficiently rapid, the overall r_1 relaxivity has contributions from C_{in}, C_{out} and $C_{internal}$.[20] Despite the fact that the relaxivity of Fe_2(L2) per molecule was higher (4.9 $mM^{-1}s^{-1}$ at 9.4T, and 5.3 $mM^{-1}s^{-1}$ at 4.7T in Table 1) than the relaxivity of Fe(L1) complexes (0.97 $mM^{-1}s^{-1}$ at 4.7 T or 1.4 $mM^{-1}s^{-1}$ at 9.4 T), loading the liposomes with these hydrophilic complexes produced liposomes with similar relaxivities for lipoB1 and lipoB2 on a per Fe basis at 2.0 (± 0.3) and 1.9 (± 0.3) mM^{-1} s^{-1} at 9.4 T for LipoB1 and lipoB2, respectively. The similarity of these r_1 relaxivity values is consistent with quenching of relaxation of intraliposomal water protons through compartmentalization effects. Such quenching has been observed for Gd(III) complexes, especially at high concentrations of contrast agent.[55] This data also supports a major contribution

to the relaxivity in both LipoB1 and LipoB2 from the Fe(III) centers present in the external liposomal layer which interact directly with the bulk water protons.[19, 20]

The larger r_1 relaxivity of LipoB1 and LipoB2 compared to LipoA is attributed to more effective extraliposomal water proton relaxation by amphiphilic Fe(III) centers. Moreover, the amphiphilic Fe(III) center is anticipated to have improved T_1 proton relaxation based on a longer rotational correlation time as it is incorporated into a large liposomal particle. The per particle r_1 relaxivity of the iron-based liposomes showed the (Figure S6) at 9,000 $mM^{-1}s^{-1}$ and 34,000 $mM^{-1}s^{-1}$ for LipoA and LipoB1 respectively. The nearly 4-fold larger r_1 relaxivity per particle for LipoB1 shows the advantage of loading liposomal core and lipid bilayer with Fe(III) complexes.

Additional studies were carried out with LipoB1 as an example of a dual-mode liposome with Fe(III) complex loaded into the liposomal interior and also the bilayer. The r_1 proton relaxivity of LipoB1 shows a slight increase in r_1 relaxivity with increasing field strength, like that observed for LipoA. In contrast, the r_2 relaxivity shows a more pronounced jump between 4.7 and 9.4 T (Table 1) as expected from the more pronounced effect of field strength on T_2 processes which is related to susceptibility contributions.[9] The relaxivity of LipoB1, like LipoA, did not change markedly over the period of three days, supporting a relatively stable liposomal formulation (Figure S7).

LipoB1 was treated with high osmolarity solutions (1200 mOsm/L) and the Z-spectrum was recorded. Unlike LipoA where there was a distinct shoulder in the Z-spectrum, the Z-spectrum of lipoB1 did not show a pronounced shoulder. However, a plot of the magnetization transfer asymmetry shows a peak at a frequency offset of 4 ppm (Figure S5). The broadening of the Z-spectrum for LipoB1 is attributed to the increased T_2 effect of the amphiphilic Fe(III) complexes in the lipid bilayer. Moreover, the Fe(III) complexes that are incorporated into the liposome are

expected to mask the CEST effect through T_1 proton relaxation. For example, conjugation of a Gd(III) complex to the external surface of a LipoCEST agent serves to quench the CEST effect.[63]

Effect of pH, temperature and serum proteins. In mouse serum, the r_1 relaxivity values of both LipoA and LipoB1 at 1.4 T increase modestly. For LipoA, the r_1 relaxivity increases from 1.0 to 1.7 $mM^{-1}s^{-1}$ (Figure S8) whereas for LipoB1 the change is from 1.7 to 2.3 $mM^{-1}s^{-1}$. This increase in relaxivity is most consistent with association of the liposomes and serum proteins. Incubation of LipoB1 with serum over a three-day period shows only small changes in relaxivity, suggesting that the liposomes remain largely intact in blood serum (Figure S9). By comparison, the proton relaxivity of free Fe(L1) complex shows little change in the presence of serum albumin consistent with only very weak interactions.[42]

The effect of temperature and pH on the relaxivity of iron-based liposomes was studied to further characterize the physical properties of the liposomes and towards applications as responsive agents. The change in relaxivity of the liposomes (LipoA and LipoB1) with pH and temperature is shown in Figure 2 and Figure S10, respectively. The Fe(III) complexes in these liposome formulations contain no inner-sphere water, so proton relaxation is mediated by second-sphere waters or, alternatively, by proton exchange.[42] The decrease in r_1 relaxivity with increasing pH for LipoB1 is consistent with acid catalyzed proton exchange contributions of the hydroxypropyl groups on the exterior of the liposome. Such proton exchange contributions to relaxivity have been observed for Gd(III) complexes with hydroxy pendants[64] and for Fe(III) aquo complex.[45] A liposome-based Gd(III) system reported previously showed a pronounced increase of the water proton relaxation rates at acidic pH.[65] For LipoA, the proton relaxivity also increases with a decrease in pH but the shape of the pH profile is convex. This profile suggests that there

are additional contributing factors such as a pH dependence of the water exchange through the liposome.

A modest temperature dependence is observed for both LipoA and LipoB1 (Figure S10). For both LipoA and LipoB, the r_1 relaxivity decreases with temperature from 24 °C to 45 °C or 50 °C, respectively. This is similar to the decrease in relaxivity with an increase in temperature that is observed for Fe(L1) and for other closed-coordination sphere Fe(III) complexes.[46] Such a decrease with increasing temperature is attributed to decreasing correlation times from rotational motion and the electronic relaxation time of the Fe(III) center.[66] However, at higher temperatures (>45°C for LipoA and > 50°C for LipoB1), the r_1 relaxivity increases with temperature. This increase suggests greater bilayer permeability to water and more rapid water exchange.[19] Cycling studies are consist with the liposome remaining largely intact at these temperatures. The relaxivity at 37°C is only slightly increased compared to initial studies as the temperature is brought back down (Figure S6). This result suggests that the enhancement in the relaxivity as temperature is increased is predominantly due to increasing the exchange rate between the extraliposomal and intraliposomal water molecules from increased liposomal membrane permeability at high temperatures.

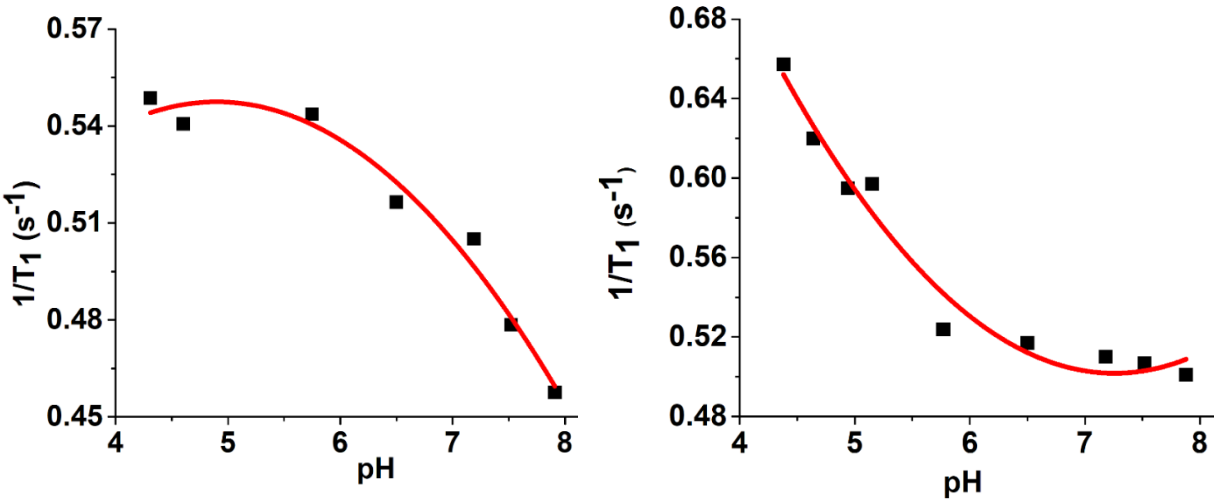

Figure 2. Plots of proton relaxation rate constants as a function of pH recorded for LipoA (Left) and LipoB1 (Right), at 34 ºC, 1.4 T.

Mice Imaging. PEGylated liposomes have a long circulation time in animals,[16] with PEGylation being key to resisting rapid sequestration by hepatobiliary elimination pathway and are important in drug delivery by liposomes. Gd-labeled PEGylated liposomes remain in the vasculature and show enhanced MRI contrast as blood pool agents. To gauge whether our iron-based liposomes would show similar characteristics in animals, LipoB1 was chosen for study to capitalize on its high per particle r_1 relaxivity. Comparison was made to Gd(DOTA). Both agents were studied in BALB/cJ mice on a small animal 4.7 T MRI scanner upon tail vein injection of the agent. The injected lipid dose was 200 mg/kg, which corresponds to 0.025 mmol iron/kg, compared to 0.05 mmol Gd(DOTA)/kg. Biodistribution and pharmacokinetic clearance of the agents in mice were monitored by MRI and are shown in Figures 3-4.

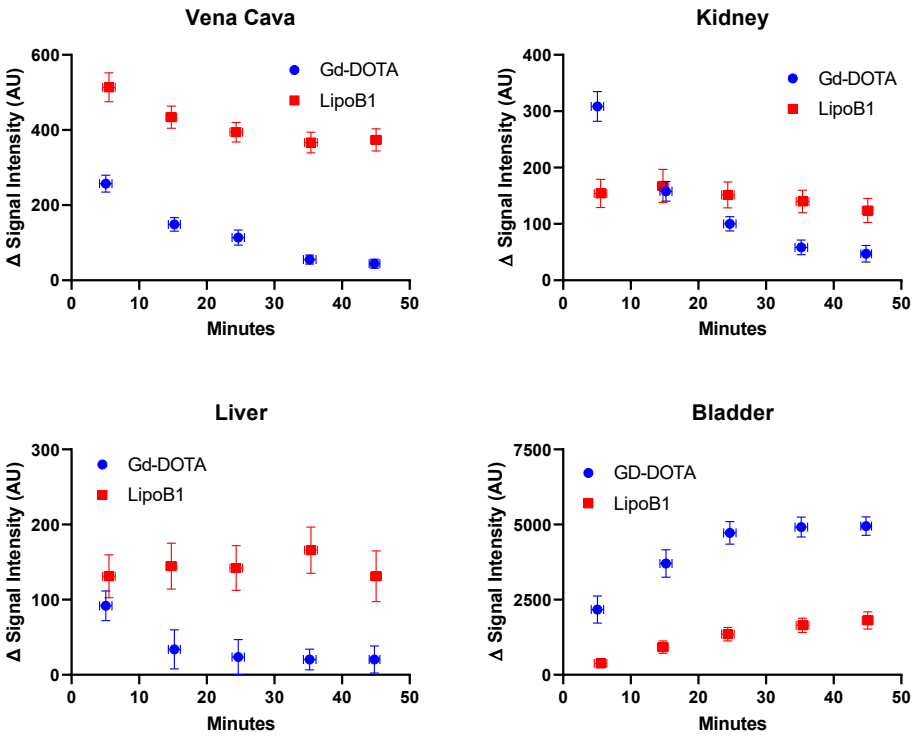

Figure 3. Changes in T_1-weighted signal intensities for LipoB1 (25 μmol [Fe]/kg versus Gd-DOTA 50 μmol[Gd]/kg over time in four different regions; blood (vena cava), kidneys, liver and urinary bladder in healthy BALB/cJ mice**.**

MR imaging shows longer retention and higher signal in the Vena Cava for LipoB1 compared to Gd(DOTA) complex as expected for a blood pool agent (Figure 3). The intensity of the signal with the iron liposomal agent compares favorably to that of Gd(DOTA), given the 2-fold lower amount injected in comparison to the Gd(III) complex. There is sustained uptake into the liver, but little gall bladder enhancement, suggesting that mostly renal clearance. This clearance differs from that shown for paramagnetic liposomes that are not surface functionalized. Non-pegylated liposomes appear predominantly in the liver.[2, 39] MR images for the experiments with LipoB1 are shown in Figure S14.

It is worth noting that the LipoB1 formulation studied here was stable in solutions containing serum for three days. However, we cannot rule out disruption of the liposome in the animal. Disruption of the phospholipid bilayer in LipoB1 would release some of the iron complexes from the interior to enhance contrast in the urinary bladder. Further studies are required to investigate this possibility. Nonetheless, initial studies are encouraging as they show enhanced and prolonged contrast of a blood vessel and predominantly renal clearance.

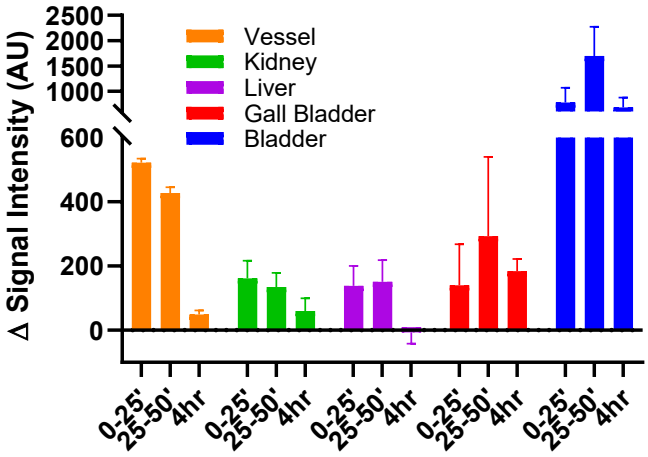

Figure 4. Changes in T_1-weighted signal intensities up to 4 h post injection for LipoB1 in tissues in healthy BALB/cJ mice at 4.7 T, at 200 mg lipids/kg. Residual enhancement in all tissues except liver was observed at 4 hours, indicating extended circulation.

CONCLUSIONS

The iron-based LipoA and LipoB liposomes feature distinct MRI probe characteristics. The LipoA agents are among the first transition metal complex-based liposomes that show both T_1 and T_2 proton relaxation enhancement as well as a modest LipoCEST effect in non-spherical liposomes. The r_1 relaxivity per iron in LipoA was quenched compared to the Fe(III) complex in the absence of liposomes, consistent with limiting water exchange rates.[55] In LipoB1 and LipoB2, the relaxivity was increased as compared to LipoA and to Fe(III) complex alone and had a much higher per particle relaxivity. This was expected based on the incorporation of an amphiphilic Fe(III) center for more effective interaction with bulk water. However, these iron-based liposomes are not as effective in proton relaxation as the best Gd(III) liposomes.[18, 67] Certainly, there is room for improvement through the incorporation of Fe(III) complexes of higher relaxivity and by variation of the amphiphilic linker as discussed below. The Fe(III) centers that are present in the external layer of LipoB produce broadened Z-spectra and also contribute to a larger T_2 proton relaxation effect, similar to studies of Ln(III) based liposomes. As a result, LipoA type formulations might serve as T_1 MRI probes whereas LipoB1 formulations might serve as T_1 or T_2 MRI probes

There are several challenges we face in further developing these liposomal iron-based agents. The first challenge is to accomplish higher loading efficiency of the complexes in the liposome interior through changes in charge and lipophilicity. The use of multinuclear complexes, as shown here, is promising for increased loading. Complexes of neutral overall charge would be anticipated to give increased liposomal loading. Higher loading efficiency would benefit studies that have the goal of releasing metal complex in response to a stimulus such as pH or temperature or for lipoCEST agents.[11, 68] Second, it is important to develop amphiphilic complexes that better anchor into the bilayer for effective interaction with bulk water. [69] This might be accomplished

by using more than one alkyl chain and by restricting the Fe(III) coordination complex to better interact with bulk water molecules in strategies similar to those published for Gd(III) complexes.[10, 18] Finally, there are other liposomal properties to vary for optimization of lipoCEST. For example, the exchange rate constant for intraliposomal water to bulk water (k_{ex}) is modulated by the composition of the liposome and may be tuned to optimize lipoCEST.[53] Moreover, the shape of the Z-spectrum, and corresponding MTR_{asym} profile depend on the magnitude of k_{ex} which varies with size of the liposome.[60]

Imaging studies of LipoB1 suggest that these liposomes hold promise as iron-based MRI probes that show blood pool agent characteristics. Steady-state enhancement of liver indicates some sequestration in the liver, perhaps due to the relatively large liposomal size, although most clearance is through a renal pathway. Further studies will investigate the role of different liposome compositions for in vivo biodistribution and pharmacokinetic clearance.

ASSOCIATED CONTENT

Supporting Information

The Supporting Information is available free of charge at:

Author contributions. The manuscript was written though contributions of all authors. All authors have read and agreed to the published version of the manuscript.

ACKNOWLEGMENTS

JRM acknowledges the NSF (CHE-2004135) for support of this work. JAS is partially supported by Roswell Park's NIH P30 grant (CA016056). The authors would like to thank the Chemistry Instrument Center (CIC), University at Buffalo. This work utilized ICP-MS and FTMS that was purchased with funding from a NSF Major Research Instrumentation Program

(NSF CHE-0959565) and National Institutes of Health (S10 RR029517). We thank Hailey Khilian for initial studies on liposomes.

Notes. JRM is a co-founder of Ferric Contrast, Inc. which develops iron-based MRI contrast agents.

REFERENCES

1. Guyon, L.; Groo, A. C.; Malzert-Freon, A., Relevant Physicochemical Methods to Functionalize, Purify, and Characterize Surface-Decorated Lipid-Based Nanocarriers. *Mol Pharmaceut* **2021,** *18* (1), 44-64.
2. Ishida, T.; Harashima, H.; Kiwada, H., Liposome clearance. *Bioscience Rep* **2002,** *22* (2), 197-224.
3. Crich, S. G.; Terreno, E.; Aime, S., Nano-sized and other improved reporters for magnetic resonance imaging of angiogenesis. *Adv Drug Deliver Rev* **2017,** *119*, 61-72.
4. Finbloom, J. A.; Sousa, F.; Stevens, M. M.; Desai, T. A., Engineering the drug carrier biointerface to overcome biological barriers to drug delivery. *Adv Drug Deliver Rev* **2020,** *167*, 89-108.
5. Langereis, S.; Geelen, T.; Grull, H.; Strijkers, G. J.; Nicolay, K., Paramagnetic liposomes for molecular MRI and MRI-guided drug delivery. *NMR Biomed* **2013,** *26* (9), 1195-1195.
6. Kneepkens, E.; Fernandes, A.; Nicolay, K.; Grull, H., Iron(III)-Based Magnetic Resonance-Imageable Liposomal T1 Contrast Agent for Monitoring Temperature-Induced Image-Guided Drug Delivery. *Invest Radiol* **2016,** *51* (11), 735-745.
7. Mulder, W. J. M.; Strijkers, G. J.; van Tilborg, G. A. F.; Griffioen, A. W.; Nicolay, K., Lipid-based nanoparticles for contrast-enhanced MRI and molecular imaging. *NMR Biomed* **2006,** *19* (1), 142-164.
8. Castelli, D. D.; Terreno, E.; Cabella, C.; Chaabane, L.; Lanzardo, S.; Tei, L.; Visigalli, M.; Aime, S., Evidence for in vivo macrophage mediated tumor uptake of paramagnetic/fluorescent liposomes. *NMR Biomed* **2009,** *22* (10), 1084-1092.
9. Mulas, G.; Ferrauto, G.; Dastru, W.; Anedda, R.; Aime, S.; Terreno, E., Insights on the relaxation of liposomes encapsulating paramagnetic Ln-based complexes. *Magn Reson Med* **2015,** *74* (2), 468-473.
10. Mulas, G.; Rolla, G. A.; Geraldes, C. F. G. C.; Starmans, L. W. E.; Botta, M.; Terreno, E.; Tei, L., Mn(II)-Based Lipidic Nanovesicles as High-Efficiency MRI Probes (vol 3, pg 2401, 2020). *Acs Appl Bio Mater* **2020,** *3* (6), 3924-3924.
11. Castelli, D. D.; Boffa, C.; Giustetto, P.; Terreno, E.; Aime, S., Design and testing of paramagnetic liposome-based CEST agents for MRI visualization of payload release on pH-induced and ultrasound stimulation. *J Biol Inorg Chem* **2014,** *19* (2), 207-214.
12. Zhang, S. Q.; Cheruku, R. R.; Dukh, M.; Tabaczynski, W.; Patel, N. J.; White, W. H.; Missert, J. R.; Spernyak, J. A.; Pandey, R. K., The Structures of Gd(III) Chelates Conjugated at

the Periphery of 3-(1'-Hexyloxy)ethyl-3-devinylpyropheophorbide-a (HPPH) Have a Significant Impact on the Imaging and Therapy of Cancer. *Chemmedchem* **2020,** *15* (21), 2058-2070.
13. Kamaly, N.; Kalber, T.; Ahmad, A.; Oliver, M. H.; So, P. W.; Herlihy, A. H.; Bell, J. D.; Jorgensen, M. R.; Miller, A. D., Bimodal paramagnetic and fluorescent liposomes for cellular and tumor magnetic resonance imaging. *Bioconjug Chem* **2008,** *19* (1), 118-129.
14. Wahsner, J.; Gale, E. M.; Rodriguez-Rodriguez, A.; Caravan, P., Chemistry of MRI Contrast Agents: Current Challenges and New Frontiers. *Chem Rev* **2019,** *119* (2), 957-1057.
15. Doan, B.-T.; Meme, S.; Beloeil, J.-C., General Principles of MRI. In *The Chemistry of Contrast Agenst in Medical Magnetic Resonance Imaging*, Merbach, A.; Helm, L.; Toth, I., Eds. Wiley: West Sussex, UK, 2013; pp 1-24.
16. Ghaghada, K. B.; Ravoori, M.; Sabapathy, D.; Bankson, J.; Kundra, V.; Annapragada, A., New Dual Mode Gadolinium Nanoparticle Contrast Agent for Magnetic Resonance Imaging. *Plos One* **2009,** *4* (10) e7628.
17. Castelli, D. D.; Terreno, E.; Longo, D.; Aime, S., Nanoparticle-based chemical exchange saturation transfer (CEST) agents. *NMR Biomed* **2013,** *26* (7), 839-49.
18. Kielar, F.; Tei, L.; Terreno, E.; Botta, M., Large Relaxivity Enhancement of Paramagnetic Lipid Nanoparticles by Restricting the Local Motions of the Gd-III Chelates. *J Am Chem Soc* **2010,** *132* (23), 7836-7837.
19. Fossheim, S. L.; Fahlvik, A. K.; Klaveness, J.; Muller, R. N., Paramagnetic liposomes as MRI contrast agents: Influence of liposomal physicochemical properties on the in vitro relaxivity. *Magn Reson Imaging* **1999,** *17* (1), 83-89.
20. Laurent, S.; Elst, L. V.; Thirifays, C.; Muller, R. N., Paramagnetic liposomes: inner versus outer membrane relaxivity of DPPC liposomes incorporating lipophilic gadolinium complexes. *Langmuir* **2008,** *24* (8), 4347-51.
21. Terreno, E.; Cabella, C.; Carrera, C.; delli castelli, D.; Mazzon, R.; Rollet, S.; Stancanello, J.; Visigalli, M.; Aime, S., From Spherical to Osmotically Shrunken Paramagnetic Liposomes: An Improved Generation of LIPOCEST MRI Agents with Highly Shifted Water Protons. *Angew. Chem. Int. Ed.* **2007** 46, 966-8.
22. Terreno, E.; Castelli, D. D.; Violante, E.; Sanders, H. M. H. F.; Sommerdijk, N. A. J. M.; Aime, S., Osmotically Shrunken LIPOCEST Agents: An Innovative Class of Magnetic Resonance Imaging Contrast Media Based on Chemical Exchange Saturation Transfer. *Chem-Eur J* **2009,** *15* (6), 1440-1448.
23. Abozeid, S. M.; Asik, D.; Sokolow, G. E.; Lovell, J. F.; Nazarenko, A. Y.; Morrow, J. R., CoII Complexes as Liposomal CEST Agents. *Angew. Chem. Int. Ed.* **2020,** *132* (29), 12191-12195.
24. Abozeid, S. M.; Snyder, E. M.; Tittiris, T. Y.; Steuerwald, C. M.; Nazarenko, A. Y.; Morrow, J. R., Inner-sphere and outer-sphere water interactions in Co (II) paraCEST agents. *Inorg Chem* **2018,** *57* (4), 2085-2095.
25. Bond, C. J.; Sokolow, G. E.; Crawley, M. R.; Burns, P. J.; Cox, J. M.; Mayilmurugan, R.; Morrow, J. R., Exploring inner-sphere water interactions of Fe (II) and Co (II) complexes of 12-membered macrocycles to develop CEST MRI probes. *Inorg Chem* **2019,** *58* (13), 8710-8719.
26. Aime, S.; Castelli, D. D.; Lawson, D.; Terreno, E., Gd-loaded liposomes as T-1, susceptibility, and CEST agents, all in one. *J Am Chem Soc* **2007,** *129* (9), 2430-+.

27. Gupta, A.; Caravan, P.; Price, W. S.; Platas-Iglesias, C.; Gale, E. M., Applications for transition-metal chemistry in contrast-enhanced magnetic resonance imaging. *Inorg Chem* **2020,** *59* (10), 6648-6678.
28. Snyder, E. M.; Asik, D.; Abozeid, S. M.; Burgio, A.; Bateman, G.; Turowski, S. G.; Spernyak, J. A.; Morrow, J. R., A Class of FeIII Macrocyclic Complexes with Alcohol Donor Groups as Effective T1 MRI Contrast Agents. *Angew Chem Int Ed* **2020,** *132* (6), 2435-2440.
29. Wang, H.; Jordan, V. C.; Ramsay, I. A.; Sojoodi, M.; Fuchs, B. C.; Tanabe, K. K.; Caravan, P.; Gale, E. M., Molecular magnetic resonance imaging using a redox-active iron complex. *J Am Chem Soc* **2019,** *141* (14), 5916-5925.
30. Kuźnik, N.; Wyskocka, M., Iron (III) contrast agent candidates for MRI: a survey of the structure–effect relationship in the last 15 years of studies. *Eur J Inorg Chem* **2016,** *2016* (4), 445-458.
31. Boehm-Sturm, P.; Haeckel, A.; Hauptmann, R.; Mueller, S.; Kuhl, C. K.; Schellenberger, E. A., Low-molecular-weight iron chelates may be an alternative to gadolinium-based contrast agents for T1-weighted contrast-enhanced MR imaging. *Radiology* **2018,** *286* (2), 537-546.
32. Bales, B. C.; Grimmond, B.; Johnson, B. F.; Luttrell, M. T.; Meyer, D. E.; Polyanskaya, T.; Rishel, M. J.; Roberts, J., Fe-HBED analogs: a promising class of iron-chelate contrast agents for magnetic resonance imaging. *Contrast Media Mol I* **2019,** *2019*.
33. Xie, J.; Haeckel, A.; Hauptmann, R.; Ray, I. P.; Limberg, C.; Kulak, N.; Hamm, B.; Schellenberger, E., Iron (III)-t CDTA derivatives as MRI contrast agents: Increased T1 relaxivities at higher magnetic field strength and pH sensing. *Magn Reson Med* **2021**, 85, 3370-3382.
34. Theil, E. C., Ferritin: The Protein Nanocage and Iron Biomineral in Health and in Disease. *Inorg Chem* **2013,** *52* (21), 12223-12233.
35. Kosman, D. J., Redox Cycling in Iron Uptake, Efflux, and Trafficking. *J Biol Chem* **2010,** *285* (35), 26729-26735.
36. Bealle, G.; Di Corato, R.; Kolosnjaj-Tabi, J.; Dupuis, V.; Clement, O.; Gazeau, F.; Wilhelm, C.; Menager, C., Ultra Magnetic Liposomes for MR Imaging, Targeting, and Hyperthermia. *Langmuir* **2012,** *28* (32), 11843-11851.
37. Malinge, J.; Geraudie, B.; Savel, P.; Nataf, V.; Prignon, A.; Provost, C.; Zhang, Y. M.; Ou, P.; Kerrou, K.; Talbot, J. N.; Siaugue, J. M.; Sollogoub, M.; Menager, C., Liposomes for PET and MR Imaging and for Dual Targeting (Magnetic Field/Glucose Moiety): Synthesis, Properties, and in Vivo Studies. *Mol Pharmaceut* **2017,** *14* (2), 406-414.
38. Lorenzato, C.; Oerlemans, C.; van Elk, M.; Geerts, W. J. C.; de Senneville, B. D.; Moonen, C.; Bos, C., MRI monitoring of nanocarrier accumulation and release using Gadolinium-SPIO co-labelled thermosensitive liposomes. *Contrast Media Mol I* **2016,** *11* (3), 184-194.
39. Schwendener, R. A.; Wuthrich, R.; Duewell, S.; Wehrli, E.; Vonschulthess, G. K., A Pharmacokinetic and Mri Study of Unilamellar Gadolinium-Dtpa-Stearate, Manganese-Dtpa-Stearate, and Iron-Dtpa-Stearate Liposomes as Organ-Specific Contrast Agents. *Invest Radiol* **1990,** *25* (8), 922-932.
40. Affram, K.; Udofot, O.; Singh, M.; Krishnan, S.; Reams, R.; Rosenberg, J.; Agyare, E., Smart thermosensitive liposomes for effective solid tumor therapy and in vivo imaging. *Plos One* **2017,** *12* (9) e0185116.

41. Asik, D.; Abozeid, S. M.; Turowski, S. G.; Spernyak, J. A.; Morrow, J. R., Dinuclear Fe(III) Hydroxypropyl-Appended Macrocyclic Complexes as MRI Probes. *Inorg Chem* **2021,** *60* (12), 8651-8664.
42. Asik, D.; Smolinski, R.; Abozeid, S. M.; Mitchell, T. B.; Turowski, S. G.; Spernyak, J. A.; Morrow, J. R., Modulating the properties of Fe (III) macrocyclic MRI contrast agents by appending sulfonate or hydroxyl groups. *Molecules* **2020,** *25* (10), 2291.
43. Palagi, L.; Di Gregorio, E.; Costanzo, D.; Stefania, R.; Cavallotti, C.; Capozza, M.; Aime, S.; Gianolio, E., Fe(deferasirox)2: An Iron(III)-Based Magnetic Resonance Imaging T1 Contrast Agent Endowed with Remarkable Molecular and Functional Characteristics. *J Am Chem Soc* **2021,** *143* (35), 14178-14188.
44. Wang, H.; Wong, A.; Lewis, L. C.; Nemeth, G. R.; Jordan, V. C.; Bacon, J. W.; Caravan, P.; Shafaat, H. S.; Gale, E. M., Rational Ligand Design Enables pH Control over Aqueous Iron Magnetostructural Dynamics and Relaxometric Properties. *Inorg Chem* **2020,** *59* (23), 17712-17721.
45. Baranyai, Z.; Carniato, F.; Nucera, A.; Horvath, D.; Tei, L.; Platas-Iglesias, C.; Botta, M., Defining the conditions for the development of the emerging class of Fe(III)-based MRI contrast agents *Chem. Sci.* **2021,** *12, 11138-11145.*
46. Kras, E.; Abozeid, S. M.; Eduardo, W.; Spernyak, J. A.; Morrow, J. R., Comparison of phosphonate, hydroxypropyl and carboxylate pendants in Fe(III) macrocyclic complexes as MRI contrast agents. *J. Inorg. Biochem.* **2021**, 225, 111594.
47. Patel, A.; Asik, D.; Snyder, E. M.; Delillo, A. E.; Cullen, P. J.; Morrow, J. R., Binding and release of Fe (III) complexes from glucan particles for delivery of T1 MRI contrast agents. *Chemmedchem* **2020**, 15, 1050-57.
48. Schubert, E. M., Utilizing the Evans Method with a Superconducting Nmr Spectrometer in the Undergraduate Laboratory. *J Chem Educ* **1992,** *69* (1), 62-62.
49. Piguet, C., Paramagnetic susceptibility by NMR: The "solvent correction" removed for large paramagnetic molecules. *J Chem Educ* **1997,** *74* (7), 815-816.
50. Silva, B. F. B.; Majzoub, R. N.; Chan, C.-L.; Li, Y.; Olsson, U.; Safinya, C. R., PEGylated cationic liposome-DNA complexation in brine is pathway-dependent. *Biochim Biophys Acta* **2014,** *1838* (1 Pt B), 398-412.
51. Mulder, W. J.; Strijkers, G. J.; Griffioen, A. W.; van Bloois, L.; Molema, G.; Storm, G.; Koning, G. A.; Nicolay, K., A liposomal system for contrast-enhanced magnetic resonance imaging of molecular targets. *Bioconjug Chem* **2004,** *15* (4), 799-806.
52. Kessel, A.; Ben-Tal, N.; May, S., Interactions of cholesterol with lipid bilayers: the preferred configuration and fluctuations. *Biophys J* **2001,** *81* (2), 643-58.
53. Chahid, B.; Vander Elst, L.; Flament, J.; Boumezbeur, F.; Medina, C.; Port, M.; Muller, R. N.; Lesieur, S., Entrapment of a neutral Tm(III)-based complex with two inner-sphere coordinated water molecules into PEG-stabilized vesicles: towards an alternative strategy to develop high-performance LipoCEST contrast agents for MR imaging. *Contrast Media Mol Imaging* **2014,** *9* (6), 391-9.
54. Ghaghada, K.; Hawley, C.; Kawaji, K.; Annapragada, A.; Mukundan, S., Jr., T1 relaxivity of core-encapsulated gadolinium liposomal contrast agents--effect of liposome size and internal gadolinium concentration. *Acad Radiol* **2008,** *15* (10), 1259-63.
55. Guenoun, J.; Doeswijk, G. N.; Krestin, G. P.; Bernsen, M. R., Compartmentalization of Gd liposomes: the quenching effect explained. *Contrast Media Mol I* **2016,** *11* (2), 106-114.

56. Li, Y.; Xie, Y.; Wang, Z.; Zang, N.; Carniato, F.; Huang, Y.; Andolina, C. M.; Parent, L. R.; Ditri, T. B.; Walter, E. D.; Botta, M.; Rinehart, J. D.; Gianneschi, N. C., Structure and Function of Iron-Loaded Synthetic Melanin. *ACS Nano* **2016,** *10* (11), 10186-10194.
57. Bertini, I.; Capozzi, F.; Luchinat, C.; Xia, Z. C., Nuclear and Electron Relaxation of $Fe(OH_2)_6^{3+}$. *J Phys Chem* **1993,** *97* (6), 1134-1137.
58. Pujales-Paradela, R.; Regueiro-Figueroa, M.; Esteban-Gómez, D.; Platas-Iglesias, C., Transition Metal-based T_1 Contrast Agents. In *Contrast Agents for MRI: Experimental Methods*, Pierre, V.; Allen, M. Eds. Royal Society: London, UK, 2018; pp 448-478.
59. Terreno, E.; Delli Castelli, D.; Violante, E.; Sanders, H. M.; Sommerdijk, N. A.; Aime, S., Osmotically shrunken LIPOCEST agents: an innovative class of magnetic resonance imaging contrast media based on chemical exchange saturation transfer. *Chemistry* **2009,** *15* (6), 1440-8.
60. Zhao, J. M.; Har-el, Y. E.; McMahon, M. T.; Zhou, J.; Sherry, A. D.; Sgouros, G.; Bulte, J. W.; van Zijl, P. C., Size-induced enhancement of chemical exchange saturation transfer (CEST) contrast in liposomes. *J Am Chem Soc* **2008,** *130* (15), 5178-84.
61. Terreno, E.; Barge, A.; Beltrami, L.; Cravotto, G.; Castelli, D. D.; Fedeli, F.; Jebasingh, B.; Aime, S., Highly shifted LIPOCEST agents based on the encapsulation of neutral polynuclear paramagnetic shift reagents. *Chem Commun* **2008,** (5), 600-602.
62. Ferrauto, G.; Delli Castelli, D.; Di Gregorio, E.; Terreno, E.; Aime, S., LipoCEST and cellCEST imaging agents: opportunities and challenges. *Wiley Interdiscip Rev Nanomed Nanobiotechnol* **2016,** *8* (4), 602-18.
63. Terreno, E.; Boffa, C.; Menchise, V.; Fedeli, F.; Carrera, C.; Castelli, D. D.; Digilio, G.; Aime, S., Gadolinium-doped LipoCEST agents: a potential novel class of dual 1H-MRI probes. *Chem Commun* **2011,** *47* (16), 4667-4669.
64. Aime, S.; Baroni, S.; Delli Castelli, D.; Brücher, E.; Fábián, I.; Serra, S. C.; Fringuello Mingo, A.; Napolitano, R.; Lattuada, L.; Tedoldi, F., Exploiting the Proton Exchange as an Additional Route to Enhance the Relaxivity of Paramagnetic MRI Contrast Agents. *Inorg Chem* **2018,** *57* (9), 5567-5574.
65. Gianolio, E.; Porto, S.; Napolitano, R.; Baroni, S.; Giovenzana, G. B.; Aime, S., Relaxometric Investigations and MRI Evaluation of a Liposome-Loaded pH-Responsive Gadolinium(III) Complex. *Inorg Chem* **2012,** *51* (13), 7210-7217.
66. Aime, S.; Botta, M.; Fasano, M.; Terreno, E., Prototropic and water-exchange processes in aqueous solutions of Gd (III) chelates. *Acc Chem Res* **1999,** *32* (11), 941-949.
67. Gugliotta, G.; Botta, M.; Tei, L., AAZTA-based bifunctional chelating agents for the synthesis of multimeric/dendrimeric MRI contrast agents. *Org Biomol Chem* **2010,** *8* (20), 4569-4574.
68. Garello, F.; Terreno, E., Sonosensitive MRI Nanosystems as Cancer Theranostics: A Recent Update. *Front Chem* **2018,** *6*.
69. Laurent, S.; Vander Elst, L.; Thirifays, C.; Muller, R. N., Relaxivities of paramagnetic liposomes: on the importance of the chain type and the length of the amphiphilic complex. *Eur Biophys J* **2008,** *37* (6), 1007-14.